J.Woisetschläger, H.Lang, B.Hampel, E.Göttlich, F.Heitmeir, (2003), *Influence of blade passing on the stator wake in a transonic turbine stage investigated by particle image velocimetry and laser vibrometry*, Proceedings 5 th European Conference on Turbomachinery, Praque, pp 1167-1174

INFLUENCE OF BLADE PASSING ON THE STATOR WAKE IN A TRANSONIC TURBINE STAGE INVESTIGATED BY PARTICLE IMAGE VELOCIMETRY AND LASER VIBROMETRY

Jakob Woisetschläger, Hermann Lang, Bernd Hampel, Emil Göttlich, Franz Heitmeir
Institute for Thermal Turbomachinery and Machine Dynamics,
Graz University of Technology
ttm@ttm.tu-graz.ac.at

ABSTRACT

The aerodynamic behaviour of stator and rotor interaction in axial flow turbines is complex and highly unsteady. Particle Image Velocimetry (PIV) and Laser Vibrometry (LV) were used to investigate the phenomena observed in a transonic turbine stage operated continuously in a cold flow test rig. While LV gave basic information on the frequency behaviour of the density fluctuations in the stator wake, stereoscopic PIV had been used for investigations of the flow fields vorticity during rotor blade passing. Phase-locking of the vortex shedding to the 7^{th} and 8^{th} harmonics of the blade passing frequency was observed.

INTRODUCTION

The wake flow in turbomachinery together with the inherent unsteadiness caused by interaction between rotor and stator has a significant impact on efficiency and performance. Wakes generated by stator rows travel downstream and interact with the succeeding rotor blades effecting pressure distribution, heat transfer and boundary layer transition (e.g. [1,2,3]) The particular problem of the influence of the blade passing effects on the vortex shedding frequency in turbines has received growing attention in recent works [4].

Detailed investigations of the flow field in rotating turbomachines have been performed using point-based measurement techniques like Laser Doppler Velocimetry (LDV) and Laser-two-focus Velocimetry (L2F) for the last few years (see e.g. [5]). In contrast to these techniques Particle Image Velocimetry (PIV) provides instantaneous velocity measurements of the whole flow field enabling a quantitative determination of vortex structures in the wake [6]. Recently, digital PIV was successfully applied to investigate the flow field of a transonic axial compressor and the diffuser region of an high speed centrifugal compressor [7,8,9] and to a transonic turbine stage [10]

On the other hand Laser-Vibrometry (LV) was applied to the turbine blade wake flow in order to obtain frequency information of density fluctuations during vortex shedding [11,12].

The object investigated in this work was a transonic turbine stage continuously operated in a cold-flow test rig [13]. Stereoscopic PIV was used for detailed flow field investigations of the structures in between stator and rotor and laser vibrometry to obtain basic information on the frequency behaviour of density fluctuations in the wake of the stator.

EXPERIMENTAL SETUP

Test turbine

In order to investigate the flow field in axial turbine stages a continuously operated, transonic test turbine facility for high pressure ratios was designed at the Institute for Thermal Turbomachinery and Machine Dynamics at Graz University of Technology [14,13]. Additional to conventional probe measurements, the test rig gave optical access to the stator rotor section. For the investigations presented herein the single stage was equipped with 24 stator blades and 36 rotor blades. For stator and rotor the chord length at mid-section was 78.9 mm and 55.9 mm, the trailing edge thickness 1.65 mm and 1,94 mm and the aspect ratio 0.7 and 1.25, respectively (see Fig.1). If not otherwise stated part-load conditions were used for the investigations, rotational speed was 9660 rpm, shaft power 1 MW, total temperature at stage inlet 367K , total pressure at inlet 250,000 Pa, pressure ratio over the stage 2.6. Conventional probing (total temperature, total pressure, static pressure) was done in the mixing chamber, upstream of the stator, between stator and rotor, downstream of the rotor and in the diffuser using PSI 9016 network scanners and National Instruments FieldPoint modules together with thermocouples and PMP 4000 pressure scanners.

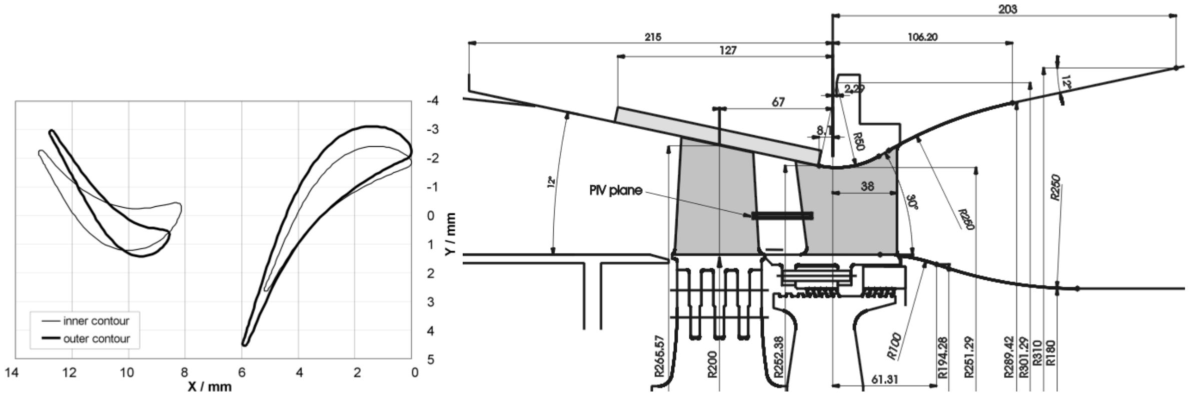

Figure 1: Test section. 24 stator blades and 36 rotor blades were used. Distances in mm, blades axes at Y=0mm.

Optical metrology

To obtain instationary data from the flow stereoscopic PIV and LV were used. The **PIV-system** used a pulsed double cavity Nd:YAG laser (120 mJ / pulse) to provide double pulses at a pulse separation of 0.7 µs. The light was guided through an articulated arm to a light-sheet optics consisting of a spherical lens (600mm focal length), a cylindrical lens (-10 mm focal length) and a prism to illuminate a plane section of the flow (see Fig.2). This section was imaged through a HERASIL glass window by two DANTEC 80C60 HiSense cameras (1280x1024 pixel) and seeded by a PALAS-AGF 5D particle generator using DEHS oil droplets of 0.7 µm nominal particle diameter introduced 500 mm upstream of the stator. A DANTEC FlowMap 110 PIV processor was used to control the recordings (one recording consisted of two images for each of the two cameras) triggered by the position of the rotor blades.

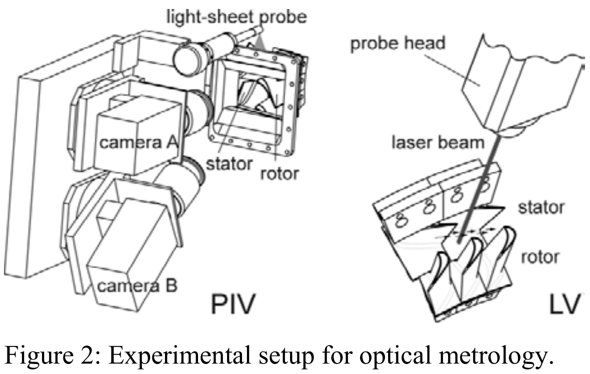

Figure 2: Experimental setup for optical metrology.

For each camera the two images were evaluated using a cross-correlation technique resulting in the vector field of displacements (displacement within the

0.7µs delay time between the two laser pulses, interrogation area size was 64x64 pixel with 50% overlap, resulting in a grid of 40x32 vectors) Finally, a range validation and a moving validation filter was applied to reject erroneous vectors [10,11].

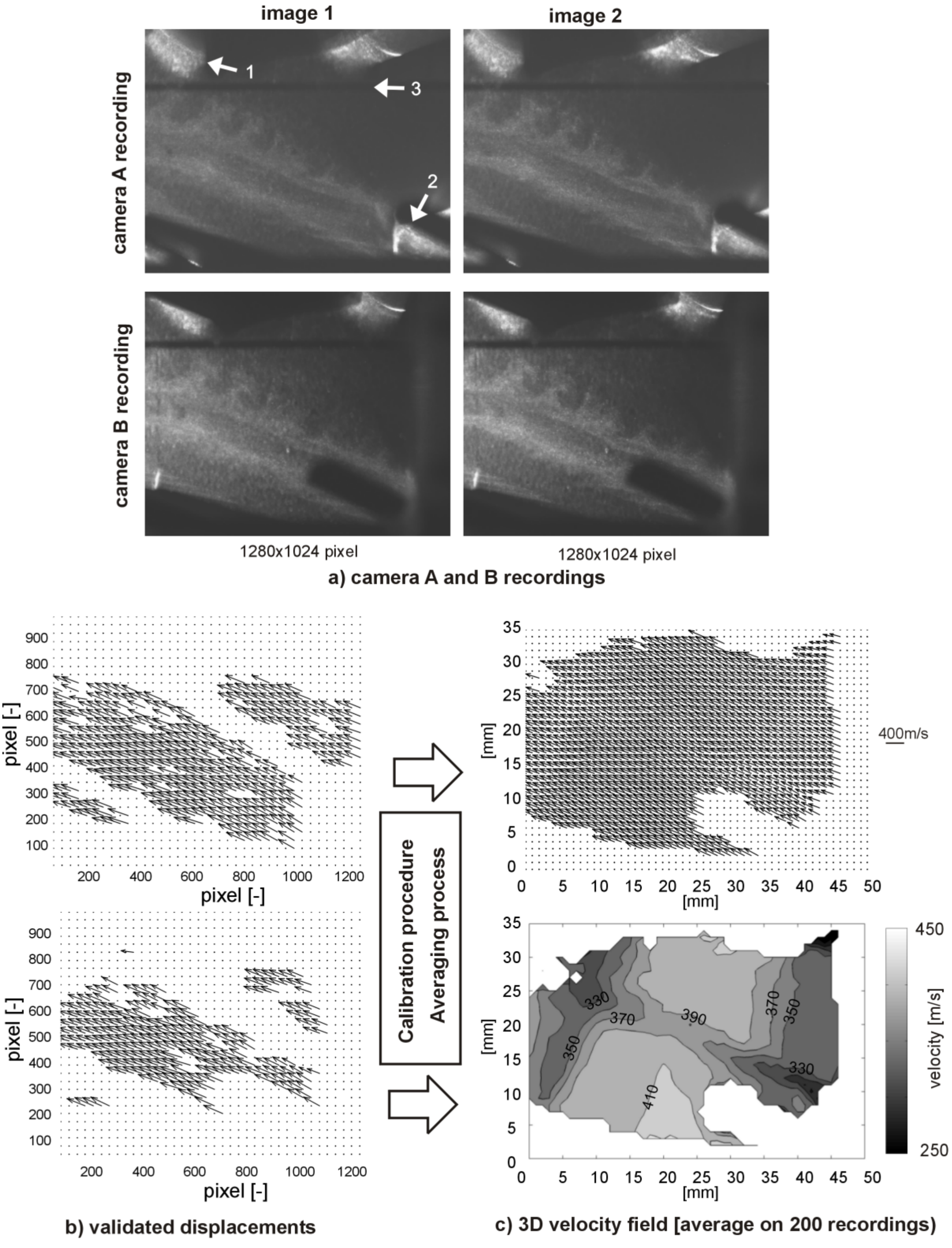

Figure 3: Evaluation of PIV recordings for a given rotor stator angle (2.4°). 1 is the position of the rotor blades, 2 is the stator trailing edge, 3 the gap between rotor and stator.

To relate the single displacements in the single recordings to physical length and combine them into a three-dimensional vector field, a calibration through the curved observation window was performed using a special calibration target (100x100 white plate with a square grid of black dots, dot spacing 2.5mm, dot size 1.5mm). This calibration procedure resulted in a polynomial function relating the single displacement fields recorded by camera A and camera B into one single velocity field for the overlap area of both cameras. [10] From these single velocity fields (180 for each rotor-stator position) mean values and vorticity fields were calculated (see Fig.3). For the vorticity the in-plane velocity components were used:

$$\omega_z = \frac{\partial v}{\partial x} - \frac{\partial u}{\partial y} \tag{1}$$

with u and v the in-plane velocities, x and y the in-plane coordinates and ω_z the vorticity with z direction perpendicular to the in-plane components, all defined in the three-dimensional velocity field.

To get information on the density fluctuations in the flow field a **Laser Vibrometer** was used (Polytec OVD 353 with OVD-3001 controller and OVD 02 velocity decoder). Widely used for vibration analysis, these interferometer type systems detect minute changes in the optical path of a laser beam emitted by and reflected back into the system. In common applications, these changes are caused by surface vibration. Here, the geometrical path was kept constant, while the density fluctuated due to turbulent motion of the fluid or pressure waves passing the laser beam. While surface vibrations occurred in the low frequency range (up to 4kHz) these density fluctuations are dominant in the frequency range above 10kHz [12,11].

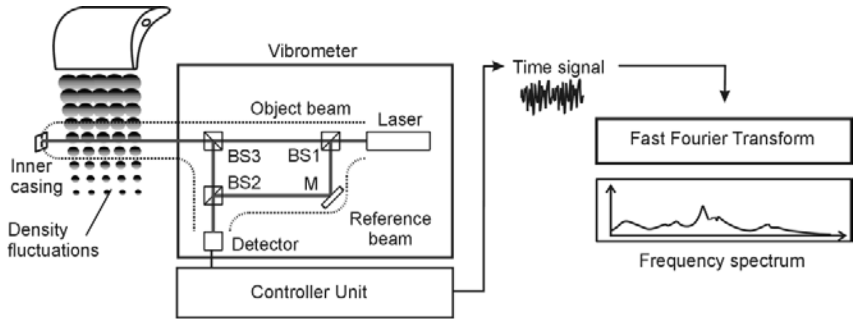

Figure 4: Principle setup of the LV. BS beam-splitter, M mirror.

For spectral analysis this signal was fed to a National Instrument 4551 dynamic signal analyser board, allowing Fast-Fourier-Transform (FFT) up to 95kHz at 950 lines or real time signal recording for two channels. For each frequency spectrum a linear rms average of up to 8000 FFTs was used, with a sampling rate of 204.8 kHz and 2048 values for each FFT.

For all investigations the laser was fixed to a position in the wake of the stator (6mm axial and 27 mm circumferential distance from the tip of the trailing edge) and reflected by the polished surface of the stator blade platform.

RESULTS

Frequency plots and time signals were recorded at different flow conditions with the LV system positioned in the wake of the stator blades. Three of these records between 3000 and 9000 rpm (3300 rpm, 7100 rpm, 8300 rpm) are presented in Fig.5, as well as one at part-load conditions at 9660 rpm. (For these measurements the beam of the LV was kept fixed to one position in the flow field of the wake as indicated by an arrow in Fig.6).

Pressure ratios and shaft power recorded are also given in Fig.5. The pressure ratio for the stator is based on the recording of the static pressure in the outer casing. From the data recorded, Reynolds-number (Re) and Strouhal-number (Str) were calculated for the stator vanes using velocity and viscosity at isentropic exit conditions [15,6]. Characteristic length for Re was the chord length of the stator blade, for Str the trailing edge thickness of the stator blade. During data recording, the pressure ratios and temperatures were continuously monitored to ensure stable conditions for each recording.

At **3300 rpm**, Re was 0.5 10^6 and vortex shedding occurred at Str 0.36. The time signal indicated more or less chaotic behaviour, no correlation with the blade passing frequency was observed. (please note the larger scaling in the time plot at 3300 rpm compared to the rest of the diagrams in Fig.5). The frequency spectrum also shows vibrational noise up to 5kHz, the blade passing frequency at 1980 Hz and three higher harmonics (two of them above 5kHz).

At **7100 rpm**, with Re 1.5 10^6 shedding occurred not only at one Strouhal-number, at least two possible frequencies at Str 0.20 and Str 0.23 were observed. The blade passing frequency gave a pronounced peak at 4260 Hz with several higher harmonics becoming visible in the spectrum of density fluctuations indicating strengthening of pressure waves propagating through the field. In the time signal all these frequencies are superimposed.

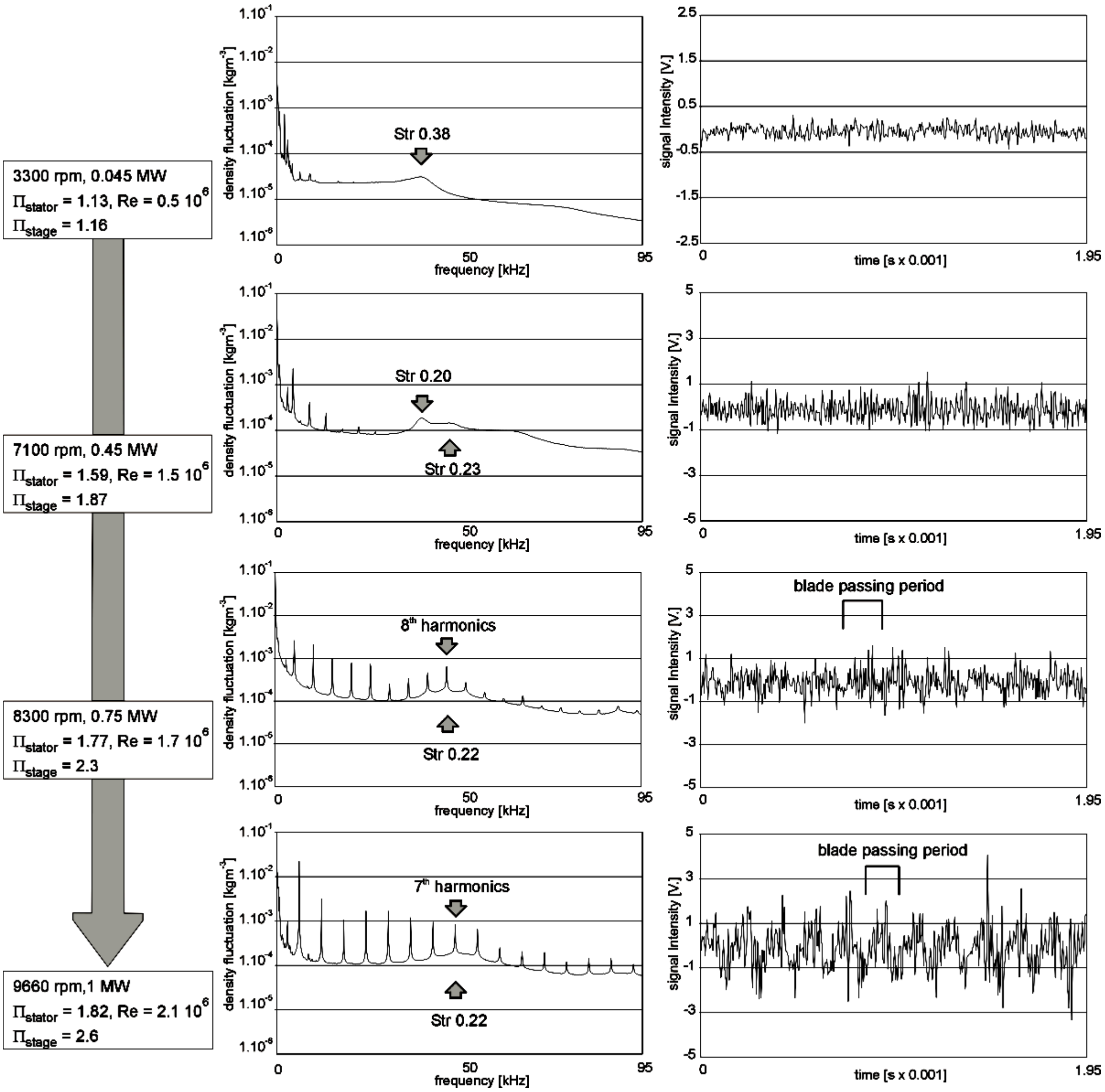

Figure 5: Frequency plots (left, density fluctuation per frequency interval over frequency) and time signals (right) of the density fluctuations in the wake as recorded by LV.

At **8300 rpm**, with Re 1.7 10^6, the flow through the stator blades was already transonic with a shock system building up. Pressure waves became dominant, seen by a strong blade passing frequency and its higher harmonics in the spectrum of density fluctuations, indicating shock reflections by the passing blades. In the time signal the blade passing period started to become visible. The shedding frequency (Str 0.22) locked to the 8^{th} harmonic of the blade passing frequency.

At **9660 rpm**, with Re 2.1 10^6, part load conditions as used for PIV recordings were reached. The shock system in the stator blades was pronounced, in some positions local Mach number equals 1.3. The pressure waves passing through the flow field clearly dominated the spectrum and the vortex shedding frequency locked to the 7^{th} harmonic of the blade passing frequency. This blade passing period and the higher harmonics can also be seen in the time signal recorded by the LV. While in some instances in time the signal was of high amplitude due to high amplitude density changes, in others the amplitude was smaller. This indicated a strong influence of the rotor on the wake flow field 'triggering' vortex shedding.

At 9660 rpm PIV recordings were carried out in a plane between rotor and stator at radius 222 mm. Fig.6 gives the velocity and the vorticity for four stator-rotor positions as recorded by PIV. The velocity is the absolute value of the three-dimensional velocity vector, the vorticity was calculated using eq. 1. Arrows in the velocity field indicate the shock, the wake and the position of the highest velocity. The arrow in the vorticity fields marks the position of LV measurements. In the vorticity fields light areas rotate counter-clockwise (suction side), dark areas clockwise (pressure side). Each of the images in Fig.6 is an average of 180 single recordings and therefore gives mean values of velocity or vorticity for these rotor-stator positions.

The passing rotor blades influenced the velocity distribution especially at the suction side of the wake. With the rotor blades a velocity defect migrated through the flow field and the wake was bent back and forth. At t=4/4T this bending is most pronounced. This coincides with the observations done with the LV system showing smaller signal amplitudes during the blade passing period (Fig.5, 9660 rpm). At these times the wake was moving away from the position where the LV was detecting density fluctuations resulting in smaller signal amplitudes in the LV.

When looking at the vorticity fields recorded by PIV (Fig.6), areas with good phase-locking between vortex shedding and rotor phase, as well as, areas with little or no phase-locking can be identified. In all positions along the wake where no clear relation in phase between the rotor passing and the vortex shedding existed, the mean value and the vortex centres were 'smeared' during the process of averaging of the 180 single recordings taken in the same stator-rotor position (see Fig.6 t=1/4T, farther downstream part of the wake). On the other hand, when there was a clear phase relation between shedding and rotor passing, the vortex field was reproducible for a given stator-rotor position and the averaging process resulted in pronounced vortex centres (e.g. Fig.6, t=4/4T).

When the shedding process was phase-locked to the rotor passing, the vorticity values observed in the averaged fields (Fig.6) never were below 60% of the values in the single images, providing clue to a highly stable vortex shedding during such intervals in the rotor passing period.

Generally, the vorticity values slightly decreased with the distance from the trailing edge. In the single recordings, as well as in the averaged fields, the pressure side vortices had higher amplitudes than those shedding from the suction side.

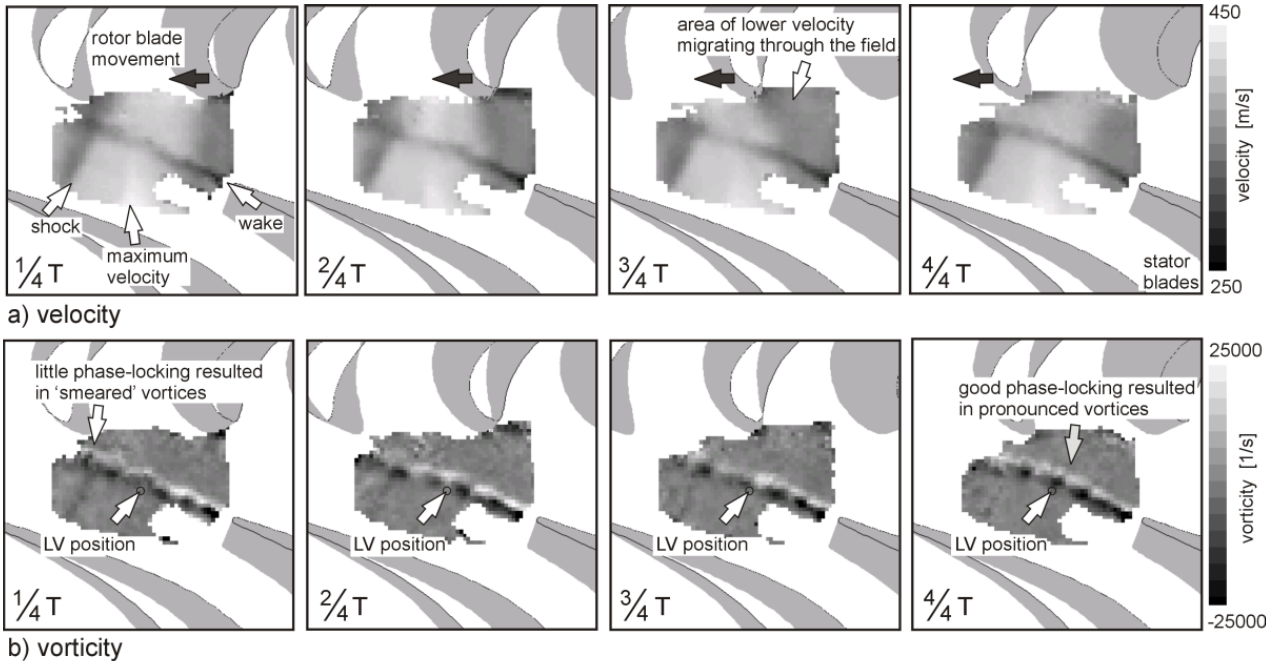

Figure 6: Velocity (above) and vorticity (below) for four stator-rotor positions as recorded by PIV (9660 rpm). For each image 180 single PIV recordings taken at the same stator-rotor position were averaged.

CONCLUSIONS

Rotor-stator interaction was experimentally investigated in a transonic turbine stage using PIV and LV. While PIV resulted in flow velocity and vorticity data for four different stator-rotor positions, the LV gave information on the density fluctuations during rotor passing observed in one point along the wake.

When the flow through the stator blades became transonic, pronounced phase-locking effects between the rotor passing and the vortex shedding were observed, as well in the density fluctuation spectra as in the PIV recordings. In the speed and pressure range investigated, the vortex shedding (Str = 0.22) locked either to the 7th or to the 8th harmonics of the blade passing frequency. Averaged PIV recordings gave information on the strong interaction between rotor passing and stator blade flow, also influencing the wake flow. During some time intervals in the rotor passing period the phase-locking was more pronounced and the shedding process more stable than during others. Therefore, a 'triggering' of the shedding by the rotor passing by seems reasonable.

ACKNOWLEDGEMENTS

This work was made possible by the Austrian Science Fund (FWF) and the Austrian Ministry for Education, Science and Culture (BMBWK) within the grant Y57-TEC "Non-intrusive measurement of turbulence in turbomachinery". The support of Dr. P. Pirker in the operation of the 3MW compressor station is also gratefully acknowledged. Graz University of Technology is member of the thematic network "PIV-NET" funded by the European Union (EU) and headed by Dr. Kompenhans, DLR. The objective of this network is to provide fast communication between designers and applicants of PIV technology.

REFERENCES

[1] Mayle, R.E. (1991), *The role of laminar-turbulent transition in gas turbine engines*, Journal of Turbomachinery, 113, 509-537

[2] Mayle, R.E., Dullenkopf, K., Schulz, A. (1998), *The turbulence that matters*, Journal of Turbomachinery, 120, 402-409

[3] Cicatelli, G., Sieverding, C.H. (1995), *A Review of the research on unsteady turbine blade wake characteristics*, AGARD PEP 85th Symposium on Loss Mechanisms and Unsteady Flows in Turbomachines, Derby, May 8-12, 1995

[4] Sondak, D.L., Dorney, D.J. (1999), *Simulation of Vortex Shedding in a Turbine Stage*, Journal of Turbomachinery, Vol. 121, 428 – 435

[5] Schodl, R., (1999), *Capabilities of Optical Point Measurement Techniques with Respect to Aero Engine Application*, RTO AVT Lecture Series on "Planar Optical Measurement Methods for Gas Turbine Components", paper 1

[6] Raffel, M., Kost, F. (1998), *Investigation of aerodynamic effects of coolant ejection at the trailing edge of a turbine blade model by PIV and pressure measurements*. Experiments in Fluids, 24, 447-461

[7] Wernet, M.P. (1999), *Application of Digital Particle Image Velocimetry to Turbomachinery*, RTO AVT Lecture Series on "Planar Optical Measurement Methods for Gas Turbine Components", paper 2

[8] Wernet, M.P. (2000), *A flow field investigation in the diffuser of a high-speed centrifugal compressor using particle image velocimetry*, Measurement Science and Technology 11 No 7, 1007-1022

[9] Wernet, M.P. (2000), *Development of digital particle image velocimetry for use in turbomachinery*, Experiments in Fluids, 28, 97-115

[10] Lang, H., Mørck, T., Woisetschläger, J. (2002), *Stereoscopic particle image velocimetry in a transonic turbine stage*, Experiments in Fluids, 32, 700-709

[11] Woisetschläger, J. , Mayrhofer, N., Hampel, B., Lang, H. *Laser-optical investigation of turbine wake flow,* submitted to Measurement Science and Technology

[12] Mayrhofer, N., Woisetschläger, J. (2001), *Frequency analysis of turbulent compressible flows by laser vibrometry*, Experiments in Fluids, 31, 153-161

[13] Erhard, J., Gehrer A., (2000), *Design and Construction of a Transonic Test-Turbine Facility*, Proceedings ASME, International Gas Turbine and Aeroengine Congress, paper 2000-GT-0480, Munich

[14] Neumayer, F., Kulhanek, G., Pirker, H.-P., Jericha, H., Seyr, A., Sanz, W. (2001), *Operational behaviour of a transonic test turbine facility*, Proceedings ASME, International Gas Turbine & Aeroengine Congress, ASME Paper No- 2001-GT-489, Orlando

[15] Bölcs, A., Suter, P. (1986), *Transsonische Turbomaschinen*, G.Braun, Karlsruhe